

# Comparison of CT Dose Reduction Algorithms in a Porcine Model

Mohammed Nazir Khan<sup>1</sup>, Idris Elbakri<sup>2</sup>, Blair Henderson<sup>1</sup>, Jeffrey Mottola<sup>1</sup>, Azeez Omotayo<sup>2</sup>

<sup>1</sup>Department of Radiology, University of Manitoba, Winnipeg, Canada

<sup>2</sup>Cancer Care Manitoba, Winnipeg, Canada

Email: nazirkhanmd@gmail.com

Received 12 October 2015; accepted 29 November 2015; published 2 December 2015

Copyright © 2015 by authors and Scientific Research Publishing Inc.

This work is licensed under the Creative Commons Attribution International License (CC BY).

<http://creativecommons.org/licenses/by/4.0/>



Open Access

---

## Abstract

The present study utilized a porcine model for qualitative and quantitative assessment of the diagnostic quality of non-contrast abdominal computed tomography (CT) images generated by Adaptive Statistical Iterative Reconstruction (ASIR, GE Healthcare, Waukesha, Wisconsin, USA), Model-Based Iterative Reconstruction (GE company name VEO), and conventional Filtered back projection (FBP) technique. **Methods:** Multiple CT whole-body scans of a freshly euthanized pig carcass were performed on a 64-slice GE CT scanner at varying noise indices (5, 10, 15, 20, 30, 37, 40, 45), and with three different algorithms (VEO, FBP, and ASIR at 30%, 50%, and 70% levels of ASIR-FBP blending). Abdominal CT images were reviewed and scored in a blinded and randomized manner by two board-certified abdominal radiologists. The task was to evaluate the clarity of the images according to a rubric involving edge sharpness, presence of artifact, anatomical clarity (assessed at four regions), and perceived diagnostic acceptability. This amounted to seven criteria, each of which was graded on a scale of 1 to 5. A weighted formula was used to calculate a composite score for each scan. **Results:** VEO outperforms ASIR and FBP by an average of 0.5 points per the scoring system used ( $p < 0.05$ ). Above a threshold noise index of 30, diagnostic acceptability is lost by all algorithms, and there is no diagnostic advantage to increasing the dose beyond a noise index of 10. Between a noise index of 25 - 30, VEO retains diagnostic acceptability, as opposed to ASIR and FBP which lose acceptability above noise index of 25. **Conclusion:** Model-based iterative reconstruction provides superior image quality and anatomical clarity at reduced radiation dosages, supporting the routine use of this technology, particularly in pediatric abdominal CT scans.

## Keywords

Computed Tomography, Dose Reduction, Iterative Reconstruction, Porcine, ASIR, VEO, FBP

---

## 1. Introduction

Healthcare in recent years has witnessed a dramatic rise in the number of computed tomography (CT) scans, which has greatly contributed to increased exposure to medical radiation. Given the evidence linking radiation exposure with carcinogenesis [1], numerous strategies to reduce radiation have been explored, including lowering tube current (mA) and potential (kVp), increased scanning pitch, the use of automated tube current modulation, and improving implementation of guidelines for avoiding unnecessary imaging. The greatest challenge with reducing CT dosage is the concomitant deterioration of image quality at lower dose levels due to increased image noise and artifacts. The development of alternative reconstruction algorithms promises to achieve lower radiation dosage while preserving acceptable image quality.

The standard reconstruction technique in use is filtered back projection (FBP), which generates a tomographic image from the raw data through an inverse Radon transform and a ramp filter. Alternative algorithms, involving iterative reconstruction, generate the radiological image through a mathematical model of the data acquisition process, thereby reducing image noise that is unlikely to represent true anatomy.

Hybrid techniques are partial iterative algorithms used in combination with FBP, while other pure model-based iterative techniques do not involve FBP. The mathematical model of all iterative techniques includes precise X-ray photon and electronic noise statistics, while model-based iterative techniques additionally take into consideration CT system optics. Historically, the lengthy processing time of iterative techniques precluded their widespread implementation. However, this is no longer a concern with modern computer technology.

Adaptive statistical iterative reconstruction (ASIR) introduced in 2009 (GE Healthcare, Waukesha, Wisconsin, USA), is a partial iterative technique involving forward projection and blending with FBP. The user determines the percentage of ASIR and FBP reconstructions in the final image. Another recent technique VEO was a model-based iterative reconstruction (MBIR) technique developed by GE Healthcare and approved for clinical use by the Food and Drug Administration (FDA) in 2011. The estimated dose reduction with ASIR is 25% - 40% and with VEO is 70% - 90% [2]. Other vendors have also introduced their own techniques including iDose and IMR (Philips Healthcare, Cleveland, Ohio, USA), IRIS, SAFIRE and ADMIRE (Siemens Healthcare, Forchheim, Germany), and AIDR-3D (Toshiba America Medical Systems, Tustin, California, USA) [3].

Since the development of these techniques, a great deal of academic research has explored comparisons between the qualities of images generated by each reconstruction algorithm. Research in phantoms has demonstrated the success of iterative reconstruction algorithms in reducing image dose without compromising image quality [4]-[6]. However, image comparisons using data from phantoms do not always approximate the clinical experience when assessing real anatomical organs and ethical limitations preclude repetitive scans to compare a wide range of techniques in a single patient. Only a few studies have utilized animal models to perform image comparisons [7]-[9]. Furthermore, many existing studies focus solely on lesion detection, which poorly approximates other clinical scenarios for which a scan may be commonly performed, such as detection of inflammatory stranding or hemorrhage surrounding a particular organ. In these cases, it is beneficial to provide a scan which has optimal clarity of the anatomical structures, and a rigorous scoring system is necessary to evaluate this.

The present study involved two abdominal radiologists using a scoring system that provided a detailed assessment of anatomical clarity in order to compare between FBP, ASIR and VEO non-contrast abdominal CT scans of a freshly euthanized porcine carcass obtained at various noise indices. In addition, quantitative assessment was also performed using contrast-to-noise measurements.

## 2. Methods

### 2.1. Ethics Approval

Following consultation with the animal care program at the University of Manitoba, a 36 kg pig carcass was obtained after it had been euthanized following laparoscopic surgery practice.

### 2.2. Image Acquisition and Scanning Protocol

Scanning was completed using a 64-slice clinical GE Discovery HD750 multi-detector CT scanner at the Bethesda Hospital in Steinbach, Manitoba. Total body CT scans were acquired helically in the craniocaudal direction with the pig in supine position with  $64 \times 0.625$  mm slices, a gantry rotation time of 600 ms, pitch of 0.984,

and tube voltage of 120 kilovolts. Reconstruction slice thickness was 1.25 mm. VEO reconstruction slice thickness is set by the system at 0.625 mm.

Scanning was conducted at eight different noise indices: 5, 10, 15, 20, 30, 37, 40 and 45. Scans were performed using three different algorithms: FBP, VEO, and ASIR (scanned with 30%, 50%, and 70% blending with FBP)—amounting to five different reconstruction methods. Five different reconstruction methods with eight different noise indices yielded a total of forty options. However, 38 scans were obtained due to the scan overheating prior to acquisition of VEO at a noise index of 37, and FBP at a noise index of 5. The scanner reported the CT dose index (CTDI<sub>vol</sub>) values in milligrays (mGy) corresponding to each noise index as displayed in **Table 1**.

### 2.3. Quantitative Image Assessment

Circular regions of interest (ROI) of 200 mm<sup>2</sup> in size were placed on corresponding abdominal CT images of the porcine model in reproducible locations within the gastric corpus and over the left paraspinal muscle. Measurements were obtained for the ROI pixel value average and standard deviation (SD). The contrast-to-noise ration (CNR) was calculated from the ratio of the difference of the pixel value averages between the two regions to the standard deviation in the two regions. A student's T-test compared the CNR values between algorithm techniques.

### 2.4. Qualitative Image Assessment

In order to evaluate the image quality, a rubric (**Table 2**) was devised for scoring each scan based on principles outlined in the European Guidelines for Quality Criteria for CT [10]. The rubric involved 7 criteria graded on a five-point scale. The criteria were edge sharpness, presence of artifact, four measures of anatomical clarity (hepatic portal veins, rectal mucosa, gastric rugae, and ureters), and overall subjective impression of diagnostic acceptability. A score of 3 was still considered diagnostically acceptable, whereas a score of 2 was deemed extremely limited, and 1 was considered nondiagnostic.

Images were uploaded onto the Agfa IMPAX system and viewed at the clinical workstation by two board-certified abdominal radiologists (B.T.H. and J.C.M.) in a blinded and randomized manner. The radiologist was given the opportunity to scroll through each scan, and score it using the aforementioned scoring rubric, without any time restrictions. The radiologist was required to complete the scoring for each scan before proceeding to the next, which was selected at random. Five of the series were selected twice, in order to assess intra-rater reliability. A weighted formula was used to generate final score for each scan as follows: 20% (sharpness/artifact) + 50% (anatomical clarity) + 30% (overall diagnostic acceptability). This weighted formula privileged the anatomical clarity in order to render the assessment more relevant to daily practice.

### 2.5. Statistical Analysis

Data analysis was performed using R statistical software in consultation with the biostatistics and epidemiology

**Table 1.** Scanner reported CTDI<sub>vol</sub> values for each noise index.

Noise index	CTDI <sub>vol</sub> (mGy)
45	1.32
40	1.58
37	1.84
30	2.66
20	5.86
15	10.39
10	20.27
5	26.92

**Table 2.** Rubric used by radiologists to score each scan.

Criteria	Score				
	1	2	3	4	5
Edge sharpness	Unacceptable	Suboptimal	Average	Above average	Excellent
Presence of artifact (streak, blotchy appearance)	Severely degraded beyond interpretation	Major degradation making interpretation difficulty	Mild degradation of image quality	Minimal artifacts apparent	No artifacts evident
Anatomical clarity:					
Hepatic portal veins	Not identified at all	First order branches somewhat distinguishable	First order branches well delineated	Second order branches well delineated	Third order branches well delineated
Rectal mucosa	Rectal lumen not identified	Rectal lumen somewhat visualized	Rectal mucosal folds barely identifiable	Rectal mucosal folds fairly distinct	Mucosa folds and serosal lining well demarcated
Gastric rugae	Gastric lumen not identified	Gastric lumen somewhat visualized	Gastric rugae partially identifiable	Gastric rugae fully visualized but folds mutually indistinct	Gastric folds mutually distinct
Ureters	Not identified at all	Proximal portion identified with difficulty	Proximal ureter well identified, mid ureter less evident	Mid ureter clearly identified, distal ureter less evident	Ureter clearly evident from UPJ to UVJ
Subjective impression overall:					
Overall diagnostic acceptability	Nondiagnostic	Extremely limited value	Likely useful for a handful of indications	Useful for many routine indications	Useful for most conceivable indications
Score = 20% (sharpness/artifact) + 50% (anatomical clarity) + 30% (overall diagnostic acceptability)					

team at the University of Manitoba. Inter-rater and intra-rater reliability was assessed by means of Bland-Altman measures. Following this, a linear regression model was generated with the mean composite score (averaged between both readers) as the outcome variable, and noise index, algorithm type, and ASIR level as the predictor variables. Algorithm type was entered as 0 for VEO and 1 for FBP and ASIR (given that conventional FBP is simply 0% ASIR), while the input for ASIR level was 0 for both FBP and VEO. This facilitated the following regression model: (m; mean composite score) – (a; algorithm type) + (b; ASIR level) + (c; noise index), where VEO (a = 0, b = 0), FBP (a = 1, b = 0), and ASIR (a = 1, b = 30, 50, or 70 depending of ASIR level).

### 3. Results

Sample images of each algorithm at a noise index of 30 are provided in [Figure 1](#).

#### 3.1. Quantitative Assessment of Images

CNR increases with dose until it reaches a plateau at a noise index of 10 and decreases afterwards, for all algorithms. The CNR for each algorithm is plotted according to noise index in [Figure 2](#).

At low doses, VEO images had the highest CNR, which increases at a lower rate with respect to dose increment. However, at the highest doses, VEO produced lower CNR values compared to ASIR50 and ASIR70. Using the Student's T-test, a statistically significant difference was identified between the CNR values for ASIR, VEO and FBP (all less than 0.05), as outlined in [Table 3](#). However, it should be noted that no significant difference (greater than 0.05) was found in CNR values for ASIR70 and VEO.

#### 3.2. Qualitative Assessment of Images

Inter-rater reliability was evaluated by means of Cohen's kappa, utilizing a composite score of 3 as the threshold for diagnostic acceptability. The observed agreement was 89.5%, and accounting for the possibility of agreement by chance, the value of Cohen's kappa was 79%. Intra-rater reliability was also evaluated for the subset of

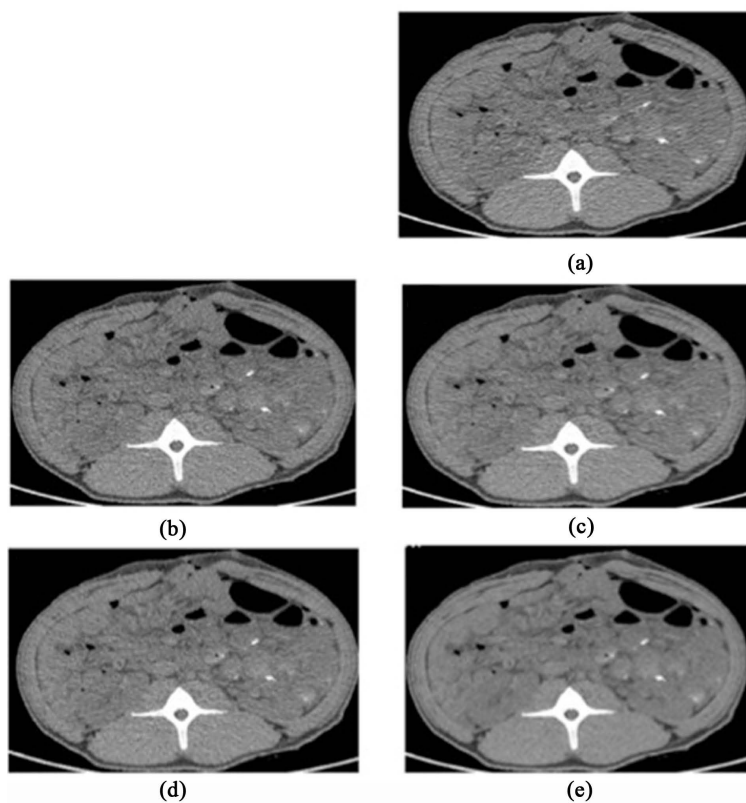


**Figure 1.** Representative images at the level of the kidneys for each algorithm at a noise index of 30. (a) Filtered back projection (FBP); (b) Adaptive statistical iteration reconstruction (ASIR) 30%; (c) ASIR 50%; (d) ASIR 70%; (e) Model-based iterative reconstruction, “VEO”.

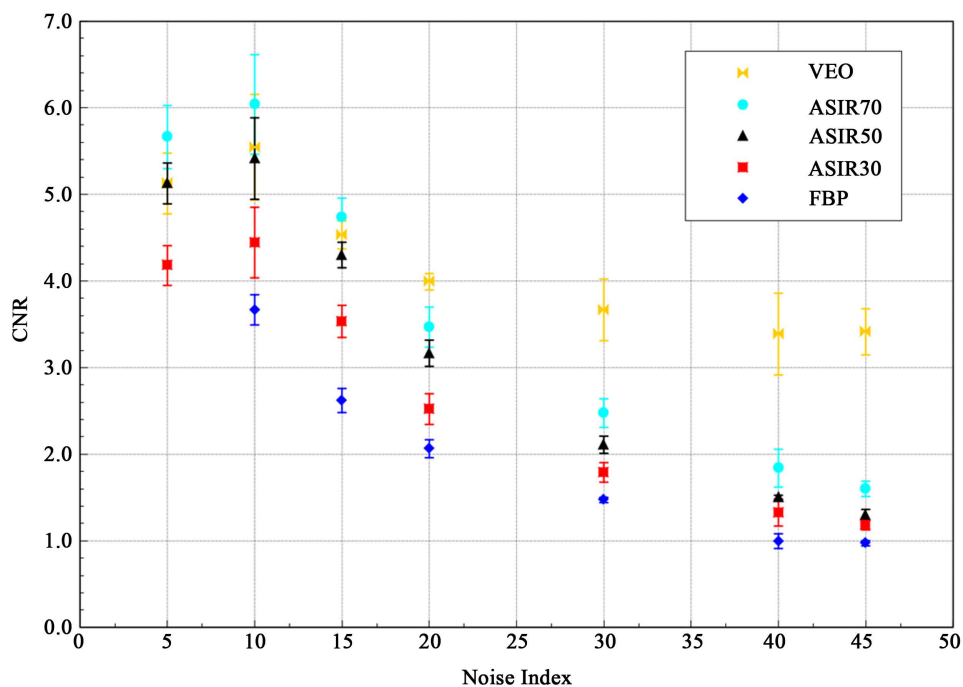


**Figure 2.** Contrast-to-Noise Ratio (CNR) calculated for each algorithm is plotted by noise index, revealing a quantitative advantage for VEO at lower doses.

**Table 3.** P-values from a student's t-test comparing CNR values between FBP, ASIR, and VEO illustrate which algorithms have a statistically significant difference.

P-values for CNR values (Student's T-test at 5% significance level)					
Algorithms	FBP	ASIR 30%	ASIR 50%	ASIR 70%	MBIR: VEO
FBP	-	0.0075	0.0101	0.0048	< 0.0001
ASIR30%	0.0075	-	0.0058	0.0014	0.0002
ASIR50%	0.0101	0.0058	-	0.0001	0.0281
ASIR70%	0.0048	0.0014	0.0001	-	0.1916
MBIR: VEO	< 0.0001	0.0002	0.0281	0.1916	-

scans read twice by B.T.H. and J.C.M., yielding kappa values of 1 for both, allowing for the sample size limitations. **Figure 3** shows the mean composite score for each algorithm as a function of noise index.

Linear regression analysis (which generated the model  $m = 5.653 - 0.534a + 0.001b - 0.086c$ ) demonstrated that 92% of all variation in the mean composite score was accounted for by the variables in the regression model (adjusted  $R^2 = 0.9191$ ). The regression model allowed for interpolation of data points for noise indices that had not been scanned, such as a noise index of 25, for instance.

The generated model indicated that both algorithm type (particularly choice of VEO instead of ASIR/FBP) and noise index were significant predictors of composite score, while the effect of ASIR over FBP was negligible at any level. Thus, in contrast to the advantage ASIR manifested in the quantitative analysis, all levels of ASIR appear indistinguishable to radiologists from same-dose FBP images. On the other hand, VEO typically outperformed ASIR and FBP by more than 0.5 points in the five-point scale. Between a noise index of 25 - 30, VEO retains diagnostic acceptability (scoring above 3 on the five-point scale), as opposed to ASIR and FBP which lose acceptability above a noise index of 25.

The data indicates that above a threshold noise index of 30, all algorithms lose diagnostic acceptability (*i.e.* fall below a score of 3-points). An upper limit threshold for dose utility was also evident. All scans acquired at a noise index of 5 were rated no better than those acquired at a noise index of 10. Therefore, there was no diagnostic advantage to increasing the dose beyond a noise index of 10.

#### 4. Discussion

The present study is quite novel in comparing MBIR, FBP, and multiple levels of ASIR blending, at multiple dosage levels. As such, the current study uniquely characterizes the dosage range in which a clinically relevant improvement in image quality is seen. The current study also uniquely permitted, without ethical constraints, the comparison of a vast assortment of scans in a real anatomical model. Another unique feature of the present investigation was the use of a composite score based on a weighted formula, which privileged the more concrete and clinically relevant components of the subjective assessment involving identification of anatomical structures.

Using CNR measurements, the present investigation revealed a quantitative advantage for VEO at low doses where image noise is prominent. Since VEO further models the intrinsic noise in images due to the photon starvation effects present at low dose levels, this leads to an improved contrast in VEO-reconstructed images compared to FBP and ASIR. At high doses where there is less photon starvation and less noise, VEO shows less relative advantage as ASIR produces images with better CNR. Consequently, improvement in image quality with VEO may be more readily apparent at low doses.

The qualitative analysis of the current study also suggests that VEO outperforms both FBP and ASIR between noise indices of 10 - 30. The characteristic pixelated blotchy appearance of VEO images was not found to negatively impact the diagnostic performance of the images generated. As has been previously noted [11], MBIR is a soft tissue reconstruction method and provides suboptimal evaluation of bone and lung anatomy, thus only soft tissue anatomical structures were evaluated in the current investigation.

A number of preceding investigations have compared dose algorithms in the clinical setting with a limited number of scans acquired in the same patient concurrently or consecutively. Many such studies suffer the limita-

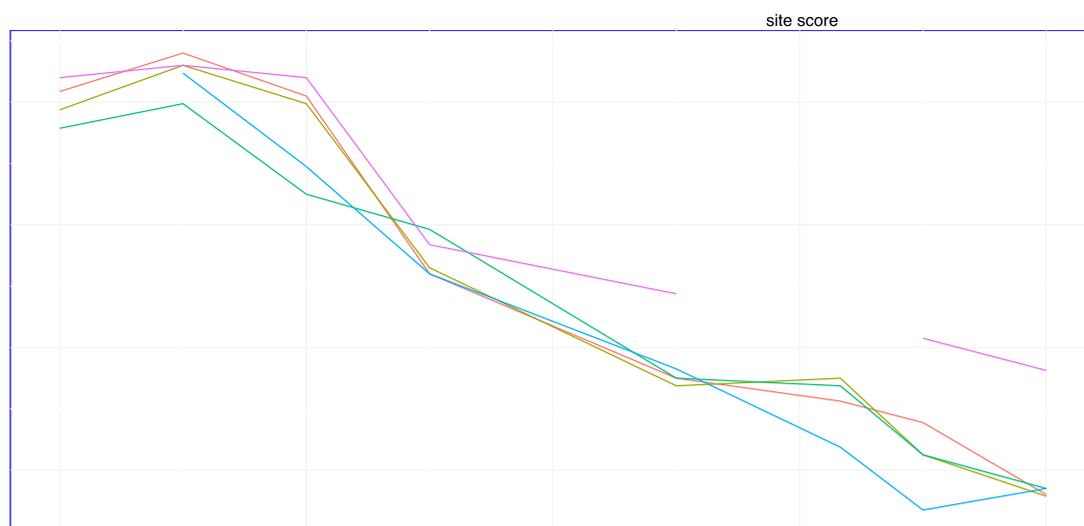


**Figure 3.** An average score was obtained for each scan using the composite score of both radiologists. The average score of each algorithm was plotted by noise level, revealing an advantage for VEO at lower doses.

tion of focusing solely on lesion detection for qualitative assessment, or are otherwise limited in comparing only a between a small range of dose-reduction techniques.

In 26 pediatric patients, an intra-individual comparison between low dose 50% ASIR-FBP blending (ASIR50) and standard dose FBP thoracic CT scans yielded a 55% dose reduction with ASIR50 without concomitant loss in diagnostic acceptability at subjective assessment [12]. In another study by Ren *et al.*, cranial CT images generated with ASIR50 allowed for a 30% dose reduction without loss of diagnostic quality when compared to FBP [13]. However, these studies did not compare between ASIR and FBP at the same dose. Our research did not demonstrate a statistically significant improvement in image quality of ASIR when compared to FBP at the same dose, which raises the question as to whether the preceding studies might have also demonstrated no discernible loss of diagnostic quality had low dose FBP been used instead of ASIR.

Our study further substantiated the results of earlier investigations suggesting a clinical advantage of MBIR over FBP and ASIR. In a study of abdominal CT scans performed for renal calculi at a single dose (noise index 50, 1.25 mm slices), MBIR demonstrated a significant improvement in subjective image quality over ASIR30, while no statistically significant difference was noted between ASIR30 and FBP [14]. The method of grading anatomical structure, utilizing the ureters was similar to the method adopted in the current study.

Katsura *et al.* compared MBIR, ASIR50, and FBP in non-contrast CT images of the cervicothoracic region of 44 patients. Objective quantitative analysis revealed significantly lower image noise in MBIR over FBP and ASIR50, and subjective image assessment accorded superior diagnostic acceptability to MBIR along with better visualization of anatomical structures, while ASIR50 did not significantly differ from FBP [15]. In a study evaluating lesion detectability, low-dose MBIR provided superior visualization of mediastinal lymph node enlargement as compared to low-dose ASIR and FBP, and demonstrated no significant difference in diagnostic performance when compared to standard dose FBP, thus permitting approximately 70% dose reduction [16]. A study performed in 25 human cadavers found that MBIR achieved a dose reduction of 82% over ASIR50 without compromise in image quality [17].

A recent study evaluated low dose CT angiography of the thoracic aorta in a live porcine model under anesthesia, comparing MBIR with FBP and ASIR50 [9]. A statistically significant improvement in subjective image quality was found with MBIR over FBP, but not with ASIR. This is again similar to the findings of the current investigation.

Other studies have demonstrated the advantages of other commercially available iterative reconstruction algorithms in a clinical setting. In a study conducted by Yamada *et al.*, standard dose (noise index 19, 2 mm slices) non-contrast thoracic CT scans in 50 patients were immediately followed by a second low dose CT scan (noise index 38, 2 mm slices) [18]. The standard dose was reconstructed with FBP and the low dose was reconstructed

with FBP, AIDR, and AIDR-3D. AIDR-3D allowed for a 64.2% reduction in dose while maintaining comparable diagnostic quality at subjective assessment.

A dual-source CT scanner was used in 53 patients to provide simultaneous intra-individual comparisons between full dose FBP with half-dose IRIS and half-dose FBP generated from a single tube detector of the scanner [19]. When compared with full dose FBP, half-dose IRIS demonstrated a 22% reduction in image noise without a statistically significant difference in lesion conspicuity, edge sharpness, visually sharp anatomical regions, and overall diagnostic acceptability.

Another study also investigated simultaneous acquisition of IRIS and FBP with arterial phase dual-source abdominal CT images in 70 patients with known or suspected liver masses. The study demonstrated that IRIS outperforms equal dose FBP in subjective measures of diagnostic acceptability, and yielded a significantly higher signal to noise ratio and contrast to noise ratio on the aorta and liver [20].

There were a number of limitations involving the present investigation. Only one vendor was evaluated in this study, and the radiologists assessed the CT of only the abdomen. The weighted formula utilized in the assessment of image quality was based on subjective judgment of the clinical relevance of the grading criteria. The 36 kg size of the pig makes it an adequate model for pediatric CT scans on a 10- to 12-year-old child, but a suboptimal model for adults. Furthermore, the porcine model did not allow for assessment of any of the pathologies commonly encountered in clinical practice. Moreover, porcine anatomy differs from human anatomy, as in the case of the five-lobed porcine liver [21]-[23]. Continued investigations with algorithms in both animal models and in human patients will afford a more accurate measure of diagnostically acceptable images.

## 5. Conclusion

The present study comparing FBP, ASIR, and VEO in a porcine model demonstrates that at reduced dosages, VEO can qualitatively outperform ASIR and FBP, with respect to clarity of anatomical structures. VEO also demonstrates a quantitative advantage on the basis of CNR measurements. Despite a quantitative difference between ASIR and FBP, image quality between these algorithms was generally indistinguishable with respect to the subjective criteria assessed. There is accumulating evidence to support routine use of model-based iterative reconstruction in the clinical setting, particularly in pediatric patients.

## Acknowledgements

For facilitating the use of the CT scanner for this project, the authors thank Bethesda Hospital, Steinbach, Manitoba, Canada. The authors thank Dr. Randy Aitken, Director of R. O. Burrell Lab, St. Boniface General Hospital, for arranging the porcine model. The authors thank Dr. Rashid Bahri, epidemiologist at Cancer Care Manitoba, for support in statistical analysis of data.

## References

- [1] Brenner, D.J. and Hall, E.J. (2007) Computed Tomography—An Increasing Source of Radiation Exposure. *The New England Journal of Medicine*, **357**, 2277-2284. <http://dx.doi.org/10.1056/NEJMra072149>
- [2] Pickhardt, P.J., Lubner, M.G., Kim, D.H., *et al.* (2012) Abdominal CT with Model-Based Iterative Reconstruction (MBIR): Initial Results of a Prospective Trial Comparing Ultralow-Dose with Standard-Dose Imaging. *American Journal of Roentgenology*, **199**, 1266-1274. <http://dx.doi.org/10.2214/AJR.12.9382>
- [3] Khawaja, R.D.A., Singh, S., Otrakji, A., *et al.* (2014) Dose Reduction in Pediatric Abdominal CT: Use of Iterative Reconstruction Techniques across Different CT Platforms. *Pediatric Radiology*, **45**, 1046-1055.
- [4] Mathieu, K.B., Ai, H., Fox, P.S., *et al.* (2014) Radiation Dose Reduction for CT Lung Cancer Screening Using ASIR and MBIR: A Phantom Study. *Journal of Applied Clinical Medical Physics*, **15**, 4515.
- [5] Rampinelli, C., Origgi, D., Vecchi, V., *et al.* (2015) Ultra-Low-Dose CT with Model-Based Iterative Reconstruction (MBIR): Detection of Ground-Glass Nodules in an Anthropomorphic Phantom Study. *Radiologia Medica*, **120**, 611-617.
- [6] Nishizawa, M., Tanaka, H., Watanabe, Y., *et al.* (2014) Model-Based Iterative Reconstruction for Detection of Subtle Hypoattenuation in Early Cerebral Infarction: A Phantom Study. *Japanese Journal of Radiology*, **33**, 26-32. <http://dx.doi.org/10.1007/s11604-014-0376-z>
- [7] Hu, M.-Q., Li, M., Liu, Z.-Y., *et al.* (2015) Image Quality Evaluation of Iterative Model Reconstruction on Low Tube Voltage (80 kVp) Coronary CT Angiography in an Animal Study. *Acta Radiologica*, pii: 0284185114568909.

- [8] Gramer, B.M., Muenzel, D., Leber, V., *et al.* (2012) Impact of Iterative Reconstruction on CNR and SNR in Dynamic Myocardial Perfusion Imaging in an Animal Model. *European Radiology*, **22**, 2654-2661. <http://dx.doi.org/10.1007/s00330-012-2525-z>
- [9] Caywood, D., Paxton, B., Boll, D., *et al.* (2014) Effects of Model-Based Iterative Reconstruction on Image Quality for Low-Dose Computed Tomographic Angiography of the Thoracic Aorta in a Swine Model. *Journal of Computer Assisted Tomography*, **39**, 196-201.
- [10] (2000) European Guidelines for Quality Criteria for Computed Tomography. European Commission, Luxembourg.
- [11] Hwang, H.J., Seo, J.B., Lee, H.J., *et al.* (2013) Low-Dose Chest Computed Tomography with Sinogram-Affirmed Iterative Reconstruction, Iterative Reconstruction in Image Space, and Filtered Back Projection: Studies on Image Quality. *Journal of Computer Assisted Tomography*, **37**, 610-617. <http://dx.doi.org/10.1097/RCT.0b013e31828f4dae>
- [12] Lee, S.H., Kim, M.J., Yoon, C.S., *et al.* (2012) Radiation Dose Reduction with the Adaptive Statistical Iterative Reconstruction (ASIR) Technique for Chest CT in Children: An Intra-Individual Comparison. *European Journal of Radiology*, **81**, e938-e943. <http://dx.doi.org/10.1016/j.ejrad.2012.06.013>
- [13] Ren, Q., Dewan, S.K., Li, M., *et al.* (2012) Comparison of Adaptive Statistical Iterative and Filtered Back Projection Reconstruction Techniques in Brain CT. *European Journal of Radiology*, **81**, 2597-2601. <http://dx.doi.org/10.1016/j.ejrad.2011.12.041>
- [14] Vardhanabhuti, V., Ilyas, S., Gutteridge, C., *et al.* (2013) Comparison of Image Quality between Filtered Back-Projection and the Adaptive Statistical and Novel Model-Based Iterative Reconstruction Techniques in Abdominal CT for Renal Calculi. *Insights Imaging*, **4**, 661-669. <http://dx.doi.org/10.1007/s13244-013-0273-5>
- [15] Katsura, M., Sato, J., Akahane, M., *et al.* (2013) Comparison of Pure and Hybrid Iterative Reconstruction Techniques with Conventional Filtered Back Projection: Image Quality Assessment in the Cervicothoracic Region. *European Journal of Radiology*, **82**, 356-360. <http://dx.doi.org/10.1016/j.ejrad.2012.11.004>
- [16] Ichikawa, Y., Kitagawa, K., Nagasawa, N., *et al.* (2013) CT of the Chest with Model-Based, Fully Iterative Reconstruction: Comparison with Adaptive Statistical Iterative Reconstruction. *BMC Medical Imaging*, **13**, 27. <http://dx.doi.org/10.1186/1471-2342-13-27>
- [17] Mueck, F.G., Roesch, S., Scherr, M., *et al.* (2015) How Low Can We Go in Contrast-Enhanced CT Imaging of the Chest? A Dose-Finding Cadaver Study Using the Model-Based Iterative Image Reconstruction Approach. *Academic Radiology*, **22**, 345-356. <http://dx.doi.org/10.1016/j.acra.2014.10.008>
- [18] Yamada, Y., Jinzaki, M., Hosokawa, T., *et al.* (2012) Dose Reduction in Chest CT: Comparison of the Adaptive Iterative Dose Reduction 3D, Adaptive Iterative Dose Reduction, and Filtered Back Projection Reconstruction Techniques. *European Journal of Radiology*, **81**, 4185-4195. <http://dx.doi.org/10.1016/j.ejrad.2012.07.013>
- [19] May, M.S., Wüst, W., Brand, M., *et al.* (2011) Dose Reduction in Abdominal Computed Tomography. *Investigative Radiology*, **46**, 465-470. <http://dx.doi.org/10.1097/RLI.0b013e31821690a1>
- [20] Wang, R., Yu, W., Wu, R., *et al.* (2012) Improved Image Quality in Dual-Energy Abdominal CT: Comparison of Iterative Reconstruction in Image Space and Filtered Back Projection Reconstruction. *American Journal of Roentgenology*, **199**, 402-406. <http://dx.doi.org/10.2214/AJR.11.7159>
- [21] Kamimura, K., Suda, T., Xu, W., *et al.* (2009) Image-Guided, Lobe-Specific Hydrodynamic Gene Delivery to Swine Liver. *Molecular Therapy*, **17**, 491-499. <http://dx.doi.org/10.1038/mt.2008.294>
- [22] Gravante, G., Ong, S.L., Metcalfe, M.S., *et al.* (2011) The Porcine Hepatic Arterial Supply, Its Variations and Their Influence on the Extracorporeal Perfusion of the Liver. *Journal of Surgical Research*, **168**, 56-61. <http://dx.doi.org/10.1016/j.jss.2009.09.050>
- [23] Martins, A.C. de A., Machado, M.A.C. and Ferraz, Á.A.B. (2008) Porcine Liver: Experimental Model for the Intra-Hepatic Glissonian Approach. *Acta Cirurgica Brasileira*, **23**, 204-207. <http://dx.doi.org/10.1590/S0102-86502008000200015>